

## EPR study of photochemical transformations of triarylmethane dyes

Vlasta Brezová<sup>a,\*</sup>, Júlia Pigošová<sup>a</sup>, Bohuslava Havlínová<sup>a</sup>, Dana Dvoranová<sup>a</sup>,  
Michal Ďurovič<sup>b</sup>

<sup>a</sup>*Faculty of Chemical and Food Technology, Slovak University of Technology in Bratislava, Radlinského 9,  
SK-812 37 Bratislava, Slovak Republic*

<sup>b</sup>*State Central Archive in Prague, Archivní 4, CZ-149 01 Prague 4, Czech Republic*

Received 30 July 2003; received in revised form 23 October 2003; accepted 27 October 2003

### Abstract

The production of reactive radical species upon irradiation ( $\lambda > 300$  nm) of six triarylmethane dyes, i.e. C.I. Basic Red 9 (42500; Basic Fuchsin), C.I. Basic Violet 3 (42555; Crystal Violet), C.I. Basic Green 4 (42000; Malachite Green Oxalate), C.I. Acid Green 16 (44025; Acid Green V), C.I. Basic Blue 11 (44040; Victoria Blue R), C.I. Acid Blue 93 (42780; Aniline Blue), as well as a phenothiazine dye C.I. Basic Blue 9 (52015; Methylene Blue) and a xanthene dye C.I. Acid Red 87 (45380; Eosin Y) in different solvents (water, ethanol, dimethylsulphoxide), and subsequently on paper substrate was investigated by means of EPR spectroscopy. The EPR experiments using spin trapping agents (5,5-dimethyl-1-pyrroline-N-oxide, DMPO and 2,3,5,6-tetramethyl nitrosobenzene, ND) showed evidence of the free radical formation in both deoxygenated and aerated systems during photoexcitation. The photooxidation processes in presence of oxygen resulted in the electron transfer generating super-oxide anion radicals (Type I process), simultaneously with energy transfer producing singlet oxygen (Type II process) confirmed by 2,2,6,6-tetramethyl-4-piperidinol (TMP).

© 2003 Elsevier Ltd. All rights reserved.

**Keywords:** Triarylmethane dyes; C.I. Basic Blue 9 (Methylene Blue); C.I. Acid Red 87 (Eosin Y); EPR spectroscopy; Spin trapping; Singlet oxygen

### 1. Introduction

Triarylmethane dyes are extensively used in textile industry for dyeing nylon, wool, silk and cotton, as well as for colouring of plastics, varnishes, waxes and oils [1,2]. Additionally, they are applied as

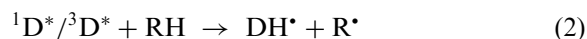
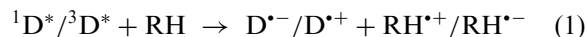
staining agents in bacteriological and histopathological methods [3]. The photocytotoxicity of triarylmethane dyes based on the reactive oxygen species production is tested intensively with the regard of their phototherapeutic potential (photodynamic therapy) [4–12]. Additionally, the triarylmethane dyes represent significant and widely utilized components of inks applied in archival documents of 19th and 20th centuries (stamps, signatures), but they are characterized by relatively

\* Corresponding author. Tel.: +4212-5932-5666; fax: +4212-5249-3198.

E-mail address: [brezova@cvtstu.cvt.stuba.sk](mailto:brezova@cvtstu.cvt.stuba.sk) (V. Brezová).

low photostability [1,2,13]. The dye photofading process is influenced by external parameters (oxygen, moisture, additives, surface properties, etc.), and the photofading rates could be quite different on substrate surfaces (paper, polymer film) comparing to photodegradation in solvents. The investigations of triphenylmethane dyes photofading in polymer films [poly (vinyl alcohol), methylcellulose, gelatin] evidenced that the photochemical process is influenced by the ability of the substrate, or residual solvent within the substrate, to donate electrons, or hydrogen atoms, to the dyes; by the ability of dyes to form aggregates; and by the chemical and physical structure of the substrates [14–20].

However, investigations of photochemical processes of dyes in homogeneous solutions may produce valuable information on the mechanism of dye photodegradation. The excited states of dye, singlet or triplet ( $^1D^*/^3D^*$ ) may interact with substrate or solvent by reductive or oxidative electron transfer and/or hydrogen abstraction process [Eqs. (1) and (2)].



In the presence of oxygen, such electron transfer from the photoexcited dye molecules may lead to the effective formation of super-oxide anion radical [4,21].

The second reaction route represents the energy transfer between dye excited triplet state and oxygen, producing singlet oxygen [Eq. (3)].



Our studies are focused on the EPR study of reactive oxygen species (hydroxyl radical, super-oxide anion radical, singlet oxygen) produced upon light exposure of aqueous, ethanolic or dimethylsulphoxide solutions of six triarylmethane dyes, as well as a phenothiazine dye C.I. Basic Blue 9 (Methylene Blue) and a xanthene dye C.I. Acid Red 87 (Eosin Y). Additionally, EPR spectroscopy was applied for the identification of  $O_2^{\bullet-}$  and  $^1O_2$  production via photoexcitation of dyes surfaced on paper substrate.

## 2. Experimental methods

### 2.1. Chemicals

Table 1 summarizes the name and synonyms, Colour Index (C.I.), structure, formula weight (FW), wavelength of absorption maximum ( $\lambda_{\max}$ ) of investigated dyes purchased from Triade (Netherlands). The polycrystalline dyes were used without further purification and were stored in dark at 5 °C in refrigerator.

The spin traps 2,3,5,6-tetramethyl nitrosobenzene (nitrosodurene, ND), 5,5-dimethyl-1-pyrroline-N-oxide (DMPO), and stable free radical 4-hydroxy-2,2,6,6-tetramethylpiperidinyloxy (TEM-POL) were obtained from Aldrich. DMPO was freshly redistilled before use and stored under argon in a freezer. The generation of singlet oxygen was evidenced by EPR using 2,2,6,6-tetramethyl-4-piperidinol (TMP) from Aldrich. Dimethylsulphoxide (DMSO) and ethanol, supplied by Fluka, were used without further purification. Redistilled water was used in the preparation of aqueous solutions. Deuterium oxide was purchased from Aldrich.

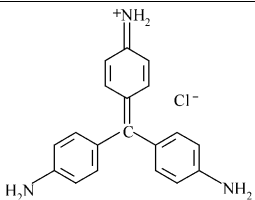
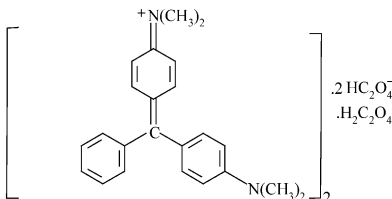
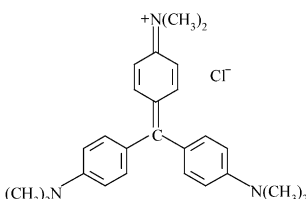
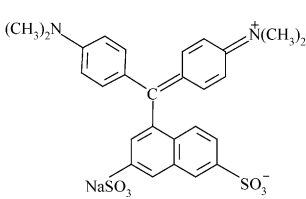
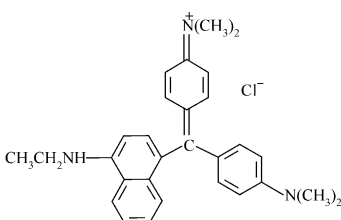
### 2.2. Procedures

The EPR spectra were measured using a Bruker 200D spectrometer (operating at X-band, using 100-kHz field modulation), which was interfaced with an Aspect 2000 computer for data acquisition, and a computer controlled Bruker EMX instrument.

The prepared solutions were carefully deoxygenated by an argon stream, or purged by air or oxygen, after which they were placed into the quartz flat cell optimized for the Bruker TM cylindrical EPR cavity. The samples were irradiated directly in the cavity of EPR spectrometer by HPA 400/30S lamp (Philips), which represents a medium-pressure metal halide source with iron and cobalt additives emitting ozone-free radiation mainly between 300 and 400 nm [22]. The lamp irradiance in UV/A region of 30 mW cm<sup>-2</sup> inside the EPR cavity was calculated by a Compact radiometer UVPS (UV Process Supply, Inc. USA). The radiation with wavelengths  $\lambda > 300$  nm was

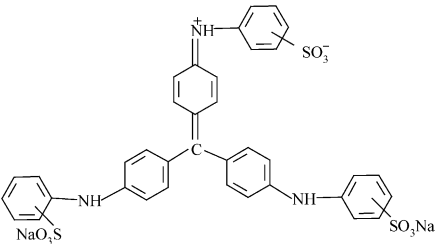
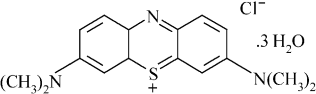
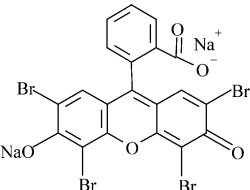
Table 1

Summarization of investigated dyes characteristics

Name, colour index (C.I.)	Structure	FW (g mol <sup>-1</sup> )	$\lambda_{\max}$ (nm)
C.I. Basic Red 9 (Basic Fuchsin, “Pararosaniline chloride”) C.I. 42500		323.83	544
C.I. Basic Green 4 (Malachite Green Oxalate) C.I. 42000		927.03	614
C.I. Basic Violet 3 (Crystal Violet, Gentian Violet) C.I. 42555		407.99	588
C.I. Acid Green 16 (Acid Green V, Naphthalene Green V) C.I. 44025		560.62	639
C.I. Basic Blue 11 (Victoria Blue R) C.I. 44040		458.05	615

(Table continued on next page)

Table 1 (continued)

C.I. Acid Blue 93 (Aniline Blue, Methyl Blue) C.I. 42780		799.81	600
C.I. Basic Blue 9 (Methylene Blue) C.I. 52015		373.90	661
C.I. Acid Red 87 (Eosin Y) C.I. 45380		691.88	514

selected by a Pyrex filter. The standard EPR experiments were performed at 290 K. Typical spectrometer settings for the series of EPR experiments were as follows: center field, 348 mT; sweep width, 6–10 mT; gain,  $5 \times 10^5$ – $2.5 \times 10^5$ ; modulation amplitude, 0.05–0.1 mT; microwave power, 20 mW; time constant, 80–200 ms; sweep time, 40–100 s. The  $g$ -values were quoted with uncertainty of  $\pm 0.0001$  by an internal reference standard marker containing 1,1-diphenyl-2-picrylhydrazyl (DPPH) built into the EPR spectrometer. The simulations of the individual components of the EPR spectra were obtained using the commercially available program *SimFonia* (Bruker). The complex experimental spin adducts EPR spectra were then fitted as the linear combinations of these individual simulations by means of a least-squares minimization procedure with the *Scientist Program* (MicroMath). The statistical parameters of calculation procedure ( $R^2$ , coefficient of determination and correlation) serve for the determination of simulation quality, i.e. harmonization of

experimental and simulated spectra. The relative concentrations of the spin adducts were calculated from the contributions of the individual spectra to experimental spectrum.

The photochemical experiments on paper were performed with Whatman 1 samples. Dye solution (50  $\mu$ l) in ethanol (1 mg/3 ml) was poured through a piece of paper (2.5 cm<sup>2</sup>), followed by 50  $\mu$ l of DMPO or TMP solution in ethanol ( $c_{\text{DMPO}} = 0.2$  mol dm<sup>-3</sup>;  $c_{\text{TMP}} = 6$  mmol dm<sup>-3</sup>), and the coloured paper was dried in dark for 15 min. The sample was then placed into a biological EPR cell with quartz window and EPR spectra were monitored in situ upon continuous irradiation.

The EPR spectra of polycrystalline dye samples were recorded at 290 K using the original single TE<sub>102</sub> (ER 4102 ST) rectangular cavity. The homogenized polycrystalline samples were placed in thin-walled quartz EPR tubes (internal diameter of 3 mm, length of 150 mm, and wall thickness about 0.1 mm) to produce cylindrical samples with identical dimensions.

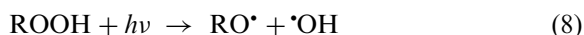
### 3. Results and discussion

#### 3.1. EPR spectra of polycrystalline dye samples

The triarylmethane dyes are naturally EPR silent compounds. However, the EPR spectra of original polycrystalline dye samples revealed presence of EPR signals, characterized by effective  $g$ -value of 2.0044, as is shown in Fig. 1. A logical explanation of these EPR signals can be rationalized as a consequence of lower photochemical and thermal stability of triarylmethane dyes. We presupposed dye autoxidation during the preparation or the storage procedure, generating hydroperoxides in accord with the generalized scheme [Eqs. (4–6)] [23,24]:



The decomposition of hydroperoxidic structures initiated by metal ions, heating or irradiation [25] resulted in the formation of reactive oxygen radical intermediates [Eqs. (7) and (8)].

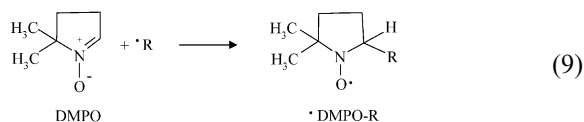


This mechanism could rationally explain the formation of oxygen-centered radical adducts monitored upon irradiation of deoxygenated dye solutions in the presence of DMPO, as will be demonstrated below.

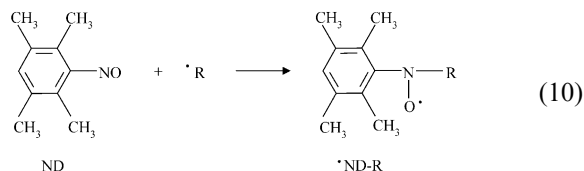
#### 3.2. Application of EPR spin trapping technique in the identification of radical species produced upon irradiation of dyes

EPR spin trapping method involves trapping of short-lived free radicals by a diamagnetic EPR silent compound (spin trap) via addition to a spin trap double bond, producing a more stable free radical product (spin adduct). Spin adducts are

paramagnetic, and have EPR spectra with hyperfine splitting constants and  $g$ -value characteristic of the type of free radical trapped [26,27]. Nitron spin traps (e.g. DMPO) scavenge free radical species via addition to a carbon located in  $\alpha$ -position relative to the nitrogen [Eq. (9)].



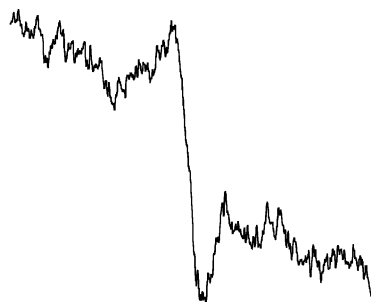
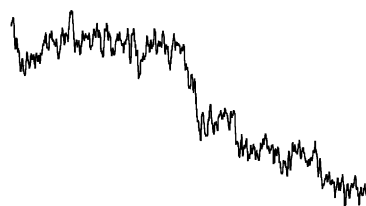
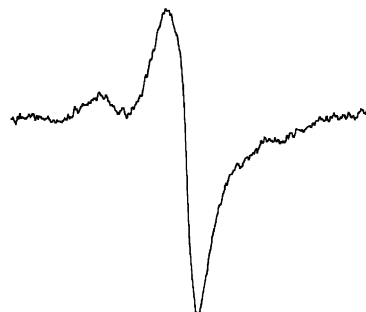
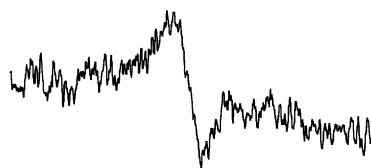
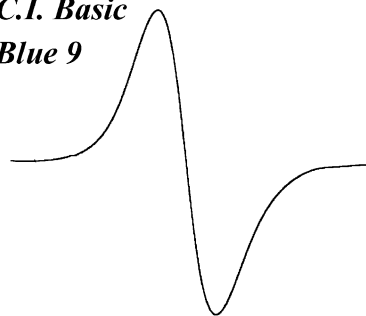
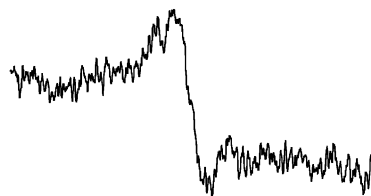
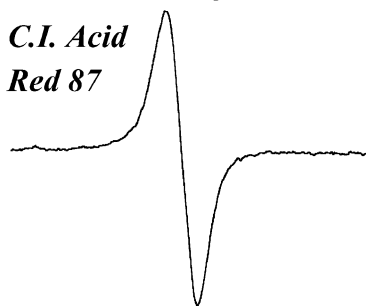
In the presence of nitroso spin trapping agents (e.g. 2,3,5,6-tetramethyl nitrosobenzene; ND) the free radicals are added directly to nitrogen [Eq. (10)], accordingly more specific information on the structure of radical trapped is obtained from the EPR spectra of the corresponding spin adducts [26,27]. The main disadvantages of ND under given experimental conditions are based on the relatively poor solubility in polar solvents, as well as on fact that trapping of oxygen-centered radical species by ND is restricted due largely to poor stability of these types of adducts [26,27].



##### 3.2.1. Aqueous dye solutions

**3.2.1.1. Oxygen.** Fig. 2 shows the time evolution of EPR signal, monitored upon continuous irradiation of aqueous oxygen-saturated solutions of C.I. Basic Blue 9 (Methylene Blue) in the presence of DMPO spin trap. The photoexcitation under given experimental conditions led to the gradual formation of four-line EPR spectrum characterized by hyperfine splittings  $a_N = 1.51$  mT,  $a_H^{\beta} = 1.49$  mT, and  $g$ -value = 2.0057. This EPR signal is attributed to DMPO spin adduct with hydroxyl radical,  ${}^{\bullet}\text{DMPO-OH}$  [27]. Fig. 3a displays experimental and simulated EPR spectra corresponding to  ${}^{\bullet}\text{DMPO-OH}$  adduct obtained upon 15 min of irradiation of C.I. Basic Blue 9 (Methylene Blue) in aqueous solution under oxygen.

The super-oxide anion radicals, primarily generated by electron transfer from the photoexcited

***C.I. Basic Red 9******C.I. Basic Blue 11******C.I. Basic Green 4******C.I. Acid Blue 93******C.I. Basic Violet 3******C.I. Basic Blue 9******C.I. Acid Green 16******C.I. Acid Red 87***

332 334 336 338 340

*Magnetic field, mT*

332 334 336 338 340

*Magnetic field, mT*

Fig. 1. EPR spectra of original polycrystalline dye samples measured at 290 K. Spectrometer settings: center field, 335.68 mT; sweep width, 10 mT; gain  $5.02 \times 10^5$ ; modulation amplitude, 0.1 mT; microwave power, 20 mW; time constant, 163.84 ms; sweep time, 41.9 s.

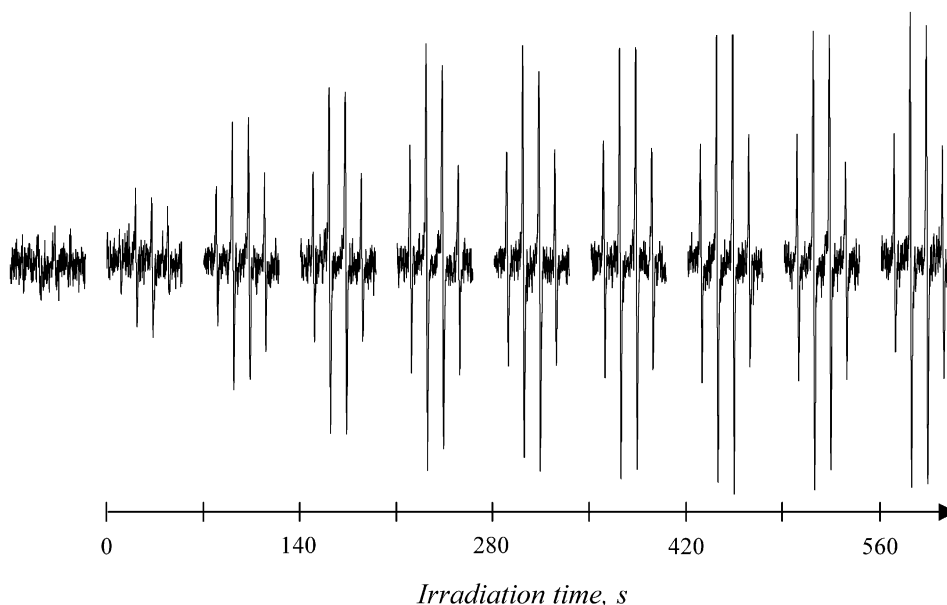
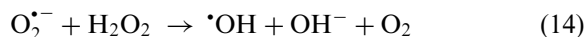
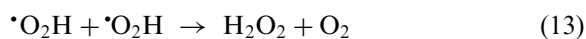


Fig. 2. Time evolution of EPR spectra (sweep width of 7 mT) monitored upon continuous irradiation ( $\lambda > 300$  nm) of aqueous oxygen-saturated solution of C.I. Basic Blue 9 (Methylene Blue) in the presence of DMPO spin trapping agent ( $c_{\text{dye}} = 8.4 \times 10^{-4}$  mol  $\text{dm}^{-3}$ ;  $c_{\text{DMPO}} = 0.01$  mol  $\text{dm}^{-3}$ ).

dye molecules to oxygen, are transformed in aqueous media by a sequence of reactions to hydroxyl radicals [Eqs. (11)–(15)] [28], which produce stable paramagnetic adduct with DMPO [27]. The addition reactions of  $\text{O}_2^{\bullet-}$  or  $\text{O}_2\text{H}^{\bullet}$  with DMPO could not be excluded, however the stability of generated  $\text{DMPO-O}_2^{\bullet-}/\text{O}_2\text{H}^{\bullet}$  spin adducts in aqueous media is low [29]. Consequently, under given experimental conditions, in the EPR spectra monitored upon irradiation predominated four-line signal corresponding to DMPO–OH adduct (Figs. 2 and 3a).



We evidenced the photoinduced production of hydroxyl radicals also in oxygen-saturated aqueous solutions upon exposure of C.I. Basic Violet 3 (Crystal Violet), C.I. Basic Green 4 (Malachite Green Oxalate) and C.I. Acid Green 16. The photochemical production of hydroxyl radicals may induce significant deterioration of dye molecules, resulting in the ink fading, as well as substrate decomposition in the concomitant presence of dye/water/oxygen factors [14–17].

Hydroxyl radicals, produced upon dye photoexcitation, represent electrophilic oxidants, and consequently, the oxidation of dye is initiated by the attack of  $\text{OH}^{\bullet}$  on an electron-rich site, most probably on the amino groups [30]. The oxidative N-demethylations of C.I. Basic Blue 9 (Methylene Blue) [31,32] and C.I. Basic Violet 3 (Crystal Violet) [33] were previously evidenced in the irradiated aqueous  $\text{TiO}_2$  suspensions. The detailed analysis of photodegradation products of Acid Orange 52 (an aminoazobenzene dye) confirmed loss of N-methyl groups probably initiated by one-electron transfer from the amino substituent by hydroxyl radicals [30], and analogous mechanism was presupposed also in the photooxidation of

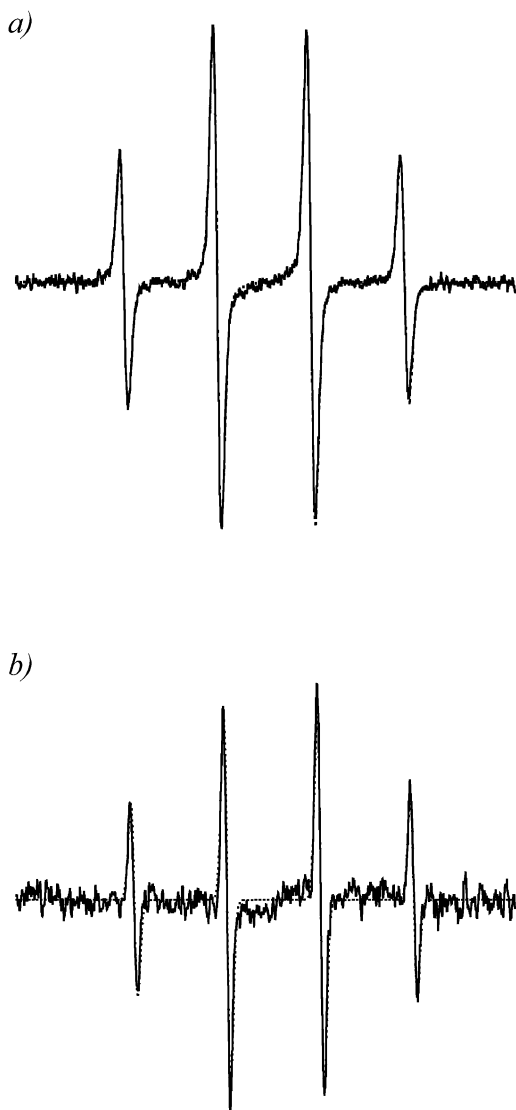


Fig. 3. Experimental (solid line) and simulated (dotted line) EPR spectra (sweep width of 7 mT) obtained upon 15 min of continuous irradiation ( $\lambda > 300$  nm) in the presence of DMPO ( $c_{\text{DMPO}} = 0.01$  mol dm $^{-3}$ ): (a) C.I. Basic Blue 9 (Methylene Blue) oxygen-saturated aqueous solution ( $c_{\text{dye}} = 8.4 \times 10^{-4}$  mol dm $^{-3}$ ); (b) C.I. Basic Violet 3 (Crystal Violet) argon-saturated aqueous solution ( $c_{\text{dye}} = 7.7 \times 10^{-4}$  mol dm $^{-3}$ ).

C.I. Basic Violet 3 (Crystal Violet) [34]. Hydrogen peroxide and hydroxyl radicals play significant role in the N-demethylation processes, e.g. the level of demethylation of C.I. Basic Violet 3 (Crystal Violet) catalyzed by horseradish perox-

idase is controlled by H $_2$ O $_2$  concentration, and analogous processes were observed for other triarylmethane dyes, as well as for C.I. Basic Blue 9 (Methylene Blue) [35,36].

**3.2.1.2. Argon.** The irradiation of de-aerated aqueous solutions of investigated dyes in the presence of DMPO caused generation of paramagnetic species only using C.I. Basic Violet 3 (Crystal Violet). Also here, in oxygen-free system, we confirmed the formation of  $\cdot\text{DMPO-OH}$  adduct (Fig. 3b). The formation of  $\cdot\text{DMPO-OH}$  in de-aerated system could be compatible with the photodecomposition of peroxidic structures present in original polycrystalline dyes [Eqs. (7) and (8)]. However, no evidence on the formation of paramagnetic species were obtained upon illumination of de-aerated aqueous solutions of C.I. Acid Blue 93, C.I. Basic Blue 9 (Methylene Blue) and C.I. Acid Red 87 (Eosin Y), i.e. dyes with the highest paramagnetic signals in the original polycrystalline samples (Fig. 1). Therefore we presupposed that in irradiated argon-saturated aqueous solutions of C.I. Basic Violet 3 (Crystal Violet),  $\cdot\text{DMPO-OH}$  adducts are formed by an alternative mechanism from the photogenerated spin trap cation-radical,  $\text{DMPO}^{\bullet+}$  [Eqs. (16) and (17)] [37].



### 3.2.2. Ethanol dye solutions

As ethanol represents an important ingredient of ink compositions, the photochemical experiments were performed in systems dye/ethanol/DMPO or dye/ethanol/ND saturated by argon or oxygen.

**3.2.2.1. Argon.** Photoexcitation of C.I. Basic Violet 3 (Crystal Violet), C.I. Basic Red 9 (Basic Fuchsin), C.I. Basic Green 4 (Malachite Green Oxalate), C.I. Basic Blue 11 (Victoria Blue R) and C.I. Acid Blue 93 dyes in deoxygenated solutions in the presence of DMPO resulted in the formation of paramagnetic signals, which were attributed to  $\cdot\text{DMPO-OC}_2\text{H}_5$ ,  $\cdot\text{DMPO-OOH}$  and  $\cdot\text{DMPO-CR}$  spin adducts, as is shown in Fig. 4.

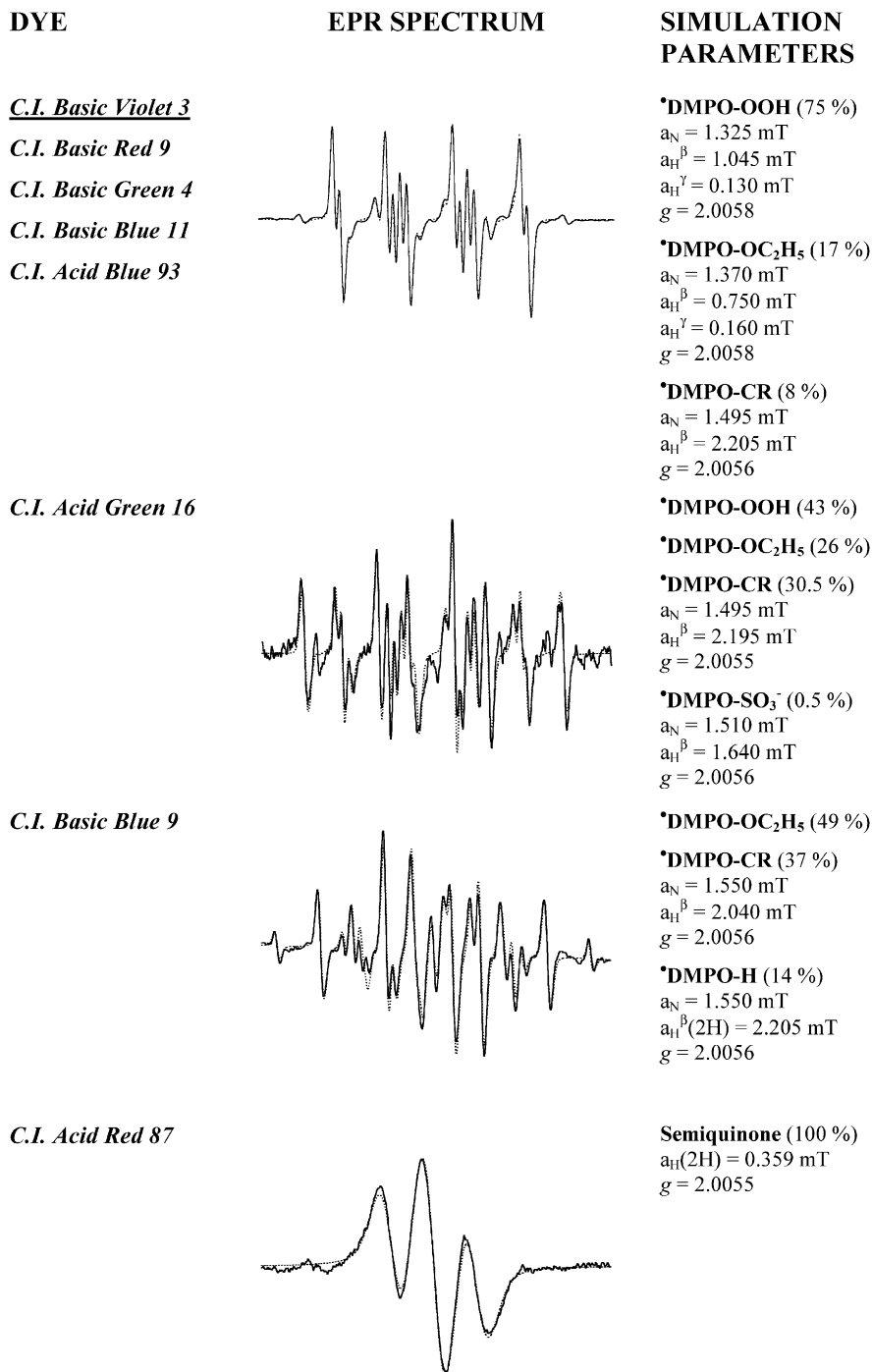
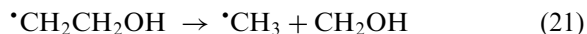
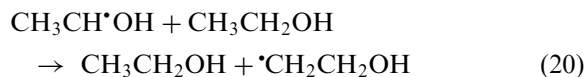
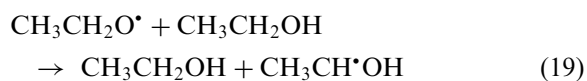


Fig. 4. Experimental (solid line) and simulated (dotted line) EPR spectra (sweep width of 7 mT) obtained upon 15 min of continuous irradiation ( $\lambda > 300 \text{ nm}$ ) in dye/ethanol/DMPO argon-saturated solutions ( $c_{\text{dye}} = (3.4\text{--}8.4) \times 10^{-4} \text{ mol dm}^{-3}$ ;  $c_{\text{DMPO}} = 0.01 \text{ mol dm}^{-3}$ ). EPR spectra in C.I. Basic Blue 9 (Methylene Blue) and C.I. Acid Red 87 (Eosin Y) solutions were measured using 8 mT and 3 mT sweep width, respectively.

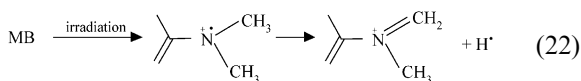
In addition to these radical species we revealed in the irradiated C.I. Acid Green 16 solutions EPR signal of low intensity corresponding to  $\bullet\text{DMPO-SO}_3^-$  spin adduct. The detection of this adduct is in good accordance with the photodesulphonation of aromatic compounds evidenced previously in our EPR experiments [38].

It should be noted here that in all systems containing triarylmethane dye/ethanol/DMPO/Ar already prior to irradiation a paramagnetic signal attributed to  $\bullet\text{DMPO-OC}_2\text{H}_5$  was identified. In the absence of light, the ethoxy radicals may be produced by the hydrogen abstraction from ethanol solvent by  $\text{ROO}\bullet$  structures [Eq. (6)]. The data obtained evidently demonstrated the important role of hydroperoxidic structures, generated in polycrystalline dyes by autoxidation processes [Eqs. (4–6)], in the photochemical processes of triarylmethane dyes, since their reactions may clarify the formation of  $\bullet\text{DMPO-O}_2\text{H}$  adduct under anaerobic conditions.

Upon irradiation, the process of hydrogen abstraction from solvent by excited triarylmethane dye molecules [Eq. (2)] led to the formation of ethoxy radicals, which are trapped by spin trapping agents, or transformed in other radical products [Eqs. (18)–(21)] [39].



Irradiation of C.I. Basic Blue 9 (Methylene Blue) (MB) under identical experimental conditions resulted in the formation of  $\bullet\text{DMPO-OC}_2\text{H}_5$ ,  $\bullet\text{DMPO-CR}$  and  $\bullet\text{DMPO-H}$  spin adducts (Fig. 4). The latter adduct may be generated by N-demethylation process [Eq. (22)], as was presupposed previously [30].



Carbon-centered adducts,  $\bullet\text{DMPO-CR}$ , monitored upon irradiation of triarylmethane dyes and C.I. Basic Blue 9 (Methylene Blue) are formed by reactions of radicals originated from solvent ( $\text{CH}_3\text{CH}\bullet\text{OH}$ ,  $\bullet\text{CH}_2\text{CH}_2\text{OH}$ ,  $\bullet\text{CH}_3$ ), or by the addition of radical species produced by the photodegradation of dyes. Application of more selective nitrosodurene spin trapping agent confirmed the photoinduced transformations of ethanol, as well as triarylmethane dyes. Paramagnetic signals monitored upon continuous irradiation of these dyes under argon in the presence of ND correspond to three spin adducts [27,39]:  $\bullet\text{ND-CH(OH)CH}_3$  ( $a_{\text{N}}=1.390$  mT,  $a_{\text{H}}^{\text{B}}=0.691$  mT;  $g=2.0057$ ),  $\bullet\text{ND-CH}_3$  ( $a_{\text{N}}=1.444$  mT,  $a_{\text{H}}^{\text{B}}(3\text{H})=1.325$  mT;  $g=2.0057$ ) and  $\bullet\text{ND-CR}$  ( $a_{\text{N}}=1.405$  mT;  $g=2.0057$ ) as is demonstrated in Fig. 5a for C.I. Basic Blue 11 (Victoria Blue R).

However, the EPR spectra measured upon irradiation of C.I. Acid Red 87 (Eosin Y) under analogous conditions were quite different (Fig. 4), while only three-line EPR signal ( $a_{\text{H}}(2\text{H})=0.359$  mT;  $g=2.0055$ ) was observed, which corresponds to the photoinduced generation of semiquinone structure of C.I. Acid Red 87 (Eosin Y) via electron and proton transfer. The photogeneration of paramagnetic semiquinone was confirmed also upon irradiation of solutions C.I. Acid Red 87 (Eosin Y)/ethanol/ND/argon. The photochemical reduction of C.I. Acid Red 87 (Eosin Y) caused the transformation of quinoidal structure of the xanthene ring into semiquinone, which is characterized by triplet EPR spectrum resulting from the hyperfine interaction of unpaired electron with two protons [40,41].

**3.2.2.2. Oxygen.** On the contrary, the irradiation of all investigated dyes in ethanol/DMPO/oxygen solutions established generation of two spin adducts, i.e.  $\bullet\text{DMPO-OOH}$  ( $a_{\text{N}}=1.320$  mT,  $a_{\text{H}}^{\text{B}}=1.045$  mT,  $a_{\text{H}}^{\text{A}}=0.130$  mT;  $g=2.0058$ ) and  $\bullet\text{DMPO-OC}_2\text{H}_5$  ( $a_{\text{N}}=1.365$  mT,  $a_{\text{H}}^{\text{B}}=0.750$  mT,  $a_{\text{H}}^{\text{A}}=0.160$  mT,  $g=2.0058$ ) as is shown in Fig. 5b for C.I. Basic Blue 11 (Victoria Blue R). These identified radical

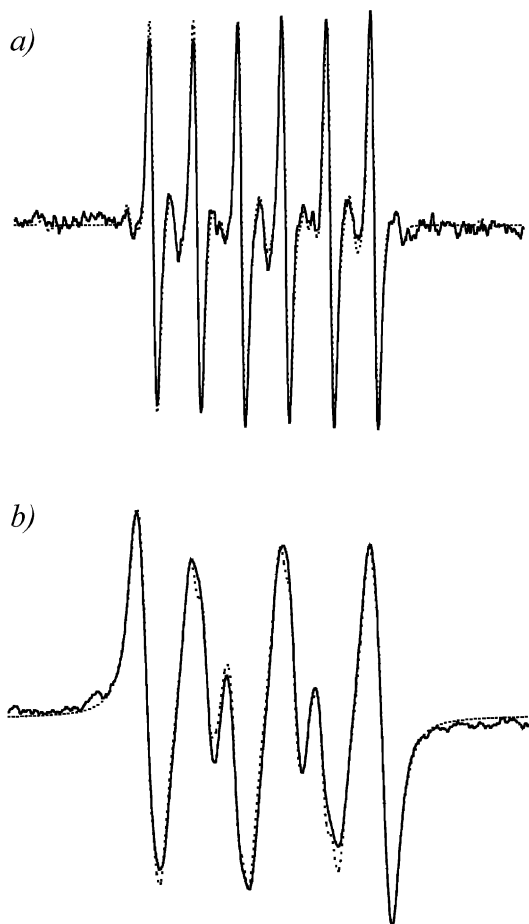


Fig. 5. Experimental (solid line) and simulated (dotted line) EPR spectra observed after 15 min of continuous irradiation ( $\lambda > 300$  nm) of C.I. Basic Blue 11 (Victoria Blue R) in ethanol solutions ( $c_{\text{dye}} = 6.8 \times 10^{-4}$  mol dm $^{-3}$ ) under: (a) argon in the presence of ND (system saturated with ND; sweep width of 10 mT); (b) oxygen in the presence of DMPO ( $c_{\text{DMPO}} = 0.01$  mol dm $^{-3}$ ; sweep width of 8 mT).

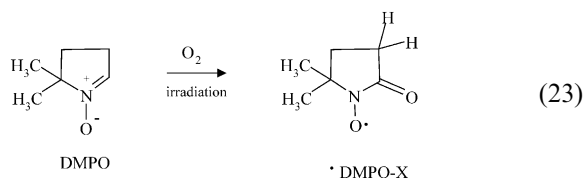
species are in good accordance with photo-oxidative electron/proton transfer mechanism (Type I process), as is described in [Eqs. (1) and (2)].

The results of EPR investigations in ethanol confirmed that photoproduct radical species, identified by spin trapping agents, originated predominantly from the solvent. Consequently, we could presuppose that in ethanol the preferential deactivation pathway of dye excited states represents interaction with solvent.

### 3.2.3. Dimethylsulphoxide dye solutions

**3.2.3.1. Oxygen.** In order to test the efficiency of  $\text{O}_2^{\cdot -}$  production upon irradiation of dyes, the photochemical experiments were performed in DMSO solvent, which is well known by its ability to stabilize super-oxide radical anions [27,42–44]. The application of DMPO spin trapping agent in DMSO solvent clearly evidenced the substantial effect of oxygen on dye photodecomposition. The formation of  $\cdot\text{DMPO-O}_2^{\cdot -}$  adduct was observed for all investigated dyes in good accordance with the proposed photooxidative mechanism [Eqs. (1) and (2)].

Fig. 6 shows the experimental and simulated EPR spectra obtained in the irradiated oxygen-saturated DMSO solutions of C.I. Basic Violet 3 (Crystal Violet) and C.I. Acid Red 87 (Eosin Y) in the presence of DMPO. The EPR spectrum presented here for C.I. Basic Violet 3 (Crystal Violet) (Fig. 6a) was simulated using hyperfine splitting constants  $a_{\text{N}} = 1.278$  mT,  $a_{\text{H}}^{\beta} = 1.040$  mT,  $a_{\text{H}}^{\gamma} = 0.142$  mT and  $g = 2.0059$ , in good accordance with the characteristics of  $\cdot\text{DMPO-O}_2^{\cdot -}$  adduct [27,42]. The equivalent EPR spectra were monitored and simulated for other dyes except for C.I. Acid Red 87 (Eosin Y) (Fig. 6b). The presence of C.I. Acid Red 87 (Eosin Y) in the irradiated system DMSO/DMPO/oxygen caused additional oxidation of  $\beta$ -hydrogen of spin trap [Eq. (23)], generating further radical product attributed to  $\cdot\text{DMPO-X}$  ( $a_{\text{N}} = 0.705$  mT,  $a_{\text{H}}^{\beta}(2\text{H}) = 0.352$  mT;  $g = 2.0066$ ) [27]. Consequently, the simulation of experimental spectra in Fig. 6b represents a linear combination of two EPR signals, i.e.  $\cdot\text{DMPO-O}_2^{\cdot -}$  (74%) and  $\cdot\text{DMPO-X}$  (24%). As C.I. Acid Red 87 (Eosin Y) behaves as effective producer of  $^1\text{O}_2$ , we concluded a singlet oxygen-induced photooxidation of DMPO, as was previously evidenced by Bilski et al. [45].



The characteristics of radical species measured upon continuous illumination of dyes in oxygenated

DMSO solutions saturated by nitrosodurene spin trap are summarized in Table 2. The photoexcitation caused the formation of spin adducts attributed to the transformations of dyes ( $\bullet\text{CR}$ ), solvent ( $\bullet\text{ND-CH}_3$ ), as well as to spin trap oxidation ( $\text{ND}^{\bullet+}$ ). The three-line EPR signal characterized by large value of nitrogen hyperfine splitting ( $a_N \sim 2.6$  mT) and lower  $g$ -value ( $g = 2.0046$ ) measured upon continuous irradiation of C.I. Basic

Green 4 (Malachite Green Oxalate), C.I. Basic Violet 3 (Crystal Violet) and C.I. Acid Blue 93 only under oxygen in the presence of ND was attributed to nitrosodurene cation-radical [46]. The assignment of radicals monitored was based on the agreement of experimental hyperfine splittings with the published data. No radical species were observed during irradiation of C.I. Basic Red 9 (Basic Fuchsin), C.I. Basic Blue 11 (Victoria Blue R), C.I. Acid Green 16 and C.I. Basic Blue 9 (Methylene Blue) under identical conditions in oxygenated DMSO/ND solutions.

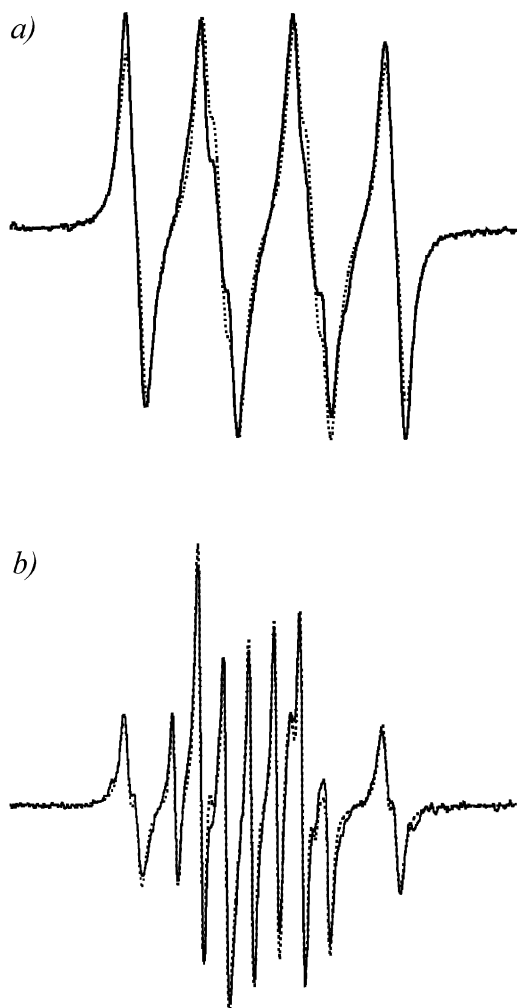


Fig. 6. Experimental (solid line) and simulated (dotted line) EPR spectra (sweep width of 7 mT) obtained upon 15 min of continuous irradiation in oxygen-saturated DMSO solutions in the presence of DMPO ( $c_{\text{DMPO}} = 0.01$  mol dm $^{-3}$ ): (a) C.I. Basic Violet 3 (Crystal Violet) ( $c_{\text{dye}} = 7.7 \times 10^{-4}$  mol dm $^{-3}$ ); (b) C.I. Acid Red 87 (Eosin Y) ( $c_{\text{dye}} = 4.5 \times 10^{-4}$  mol dm $^{-3}$ ).

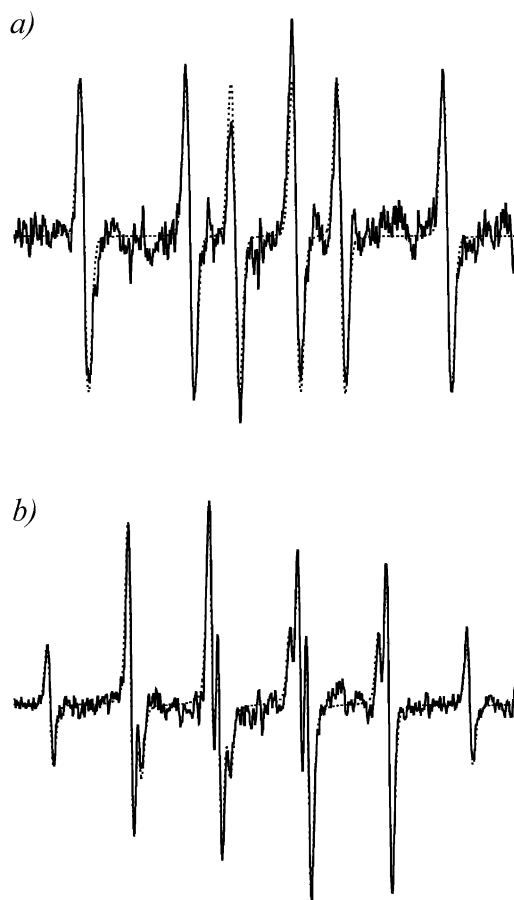


Fig. 7. Experimental (solid line) and simulated (dotted line) EPR spectra observed after 15 min of continuous irradiation ( $\lambda > 300$  nm) of C.I. Basic Violet 3 (Crystal Violet) in argon-saturated DMSO solutions ( $c_{\text{dye}} = 7.7 \times 10^{-4}$  mol dm $^{-3}$ ) in the presence of spin trapping agent: (a) DMPO ( $c_{\text{DMPO}} = 0.01$  mol dm $^{-3}$ ; sweep width of 7 mT); (b) ND (system saturated with ND; sweep width of 8 mT).

Table 2

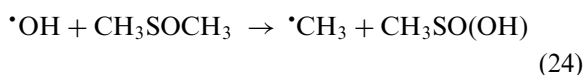
Simulation parameters of EPR spectra for nitrosodurene spin adducts obtained after 15 min of continuous irradiation ( $\lambda > 300$  nm) in oxygenated DMSO solutions saturated with spin trapping agent

Dye	ND spin adduct	Hyperfine splittings (mT)	g-value	Relative concentration (%)	Reference
C.I. Basic Green 4 (Malachite Green Oxalate)	ND• <sup>+</sup>	$a_N = 2.577$	2.0046	100	[46]
C.I. Basic Violet 3 (Crystal Violet)	•ND–CR	$a_N = 1.174$	2.0057	10.3	[27,39,46,47]
	ND• <sup>+</sup>	$a_N = 2.600$	2.0046	89.7	[46]
C.I. Acid Blue 93	•ND–CR	$a_N = 1.160$	2.0057	44.2	[27,39,46,47]
	ND• <sup>+</sup>	$a_N = 2.600$	2.0046	53.3	[46]
	•ND–CHR	$a_N = 1.160$ $a_H^B = 0.464$	2.0056	2.5	[27,39,48]
C.I. Acid Red 87 (Eosin Y)	•ND–CR	$a_N = 1.162$	2.0057	71.7	[27,39,46,47]
	ND• <sup>+</sup>	$a_N = 2.610$	2.0046	22.8	[46]
	•ND–CH <sub>3</sub>	$a_N = 1.410$ $a_H^B(3H) = 1.305$	2.0056	5.5	[27,39,46,47]

3.2.3.2. *Argon*. The illumination of investigated dyes in experimental systems dye/DMSO/DMPO/argon and dye/DMSO/ND/argon resulted in the formation of paramagnetic species, which were identified as the corresponding spin trap adducts, e.g. •DMPO–O<sub>2</sub><sup>•−</sup>, •DMPO–CR, •DMPO–SR, •DMPO–OR, •DMPO–NR, •ND–CH<sub>3</sub>, •ND–CR and semiquinone radical of C.I. Acid Red 87 (Eosin Y).

Fig. 7 shows the experimental and simulated EPR spectra monitored upon continuous irradiation of C.I. Basic Violet 3 (Crystal Violet) in de-aerated DMSO solution in the presence of DMPO (Fig. 7a) and ND (Fig. 7b). Tables 3 and 4 summarize the characteristics of EPR spectra used in the simulations of experimental spectra. The type of radical species identified upon photoexcitation under inert atmosphere was significantly dependent on dye structure, and the dominant effect plays the character and number of substitutions on triarylmethane core. Again here, we observed the formation of super-oxide anion radical adducts •DMPO–O<sub>2</sub><sup>•−</sup>, as well as •DMPO–OR under strictly deoxygenated conditions (Table 3). The photochemical transformation of hydroperoxidic structures may be a reasonable explanation of O<sub>2</sub><sup>•−</sup> and •OR species formation. Methyl radicals, unambiguously identified using ND spin trapping agent, are produced most probably via reaction of photogenerated hydroxyl radicals [Eq.

(8)] with DMSO solvent [Eq. (24)] [44,51], since this radical species was trapped almost in all argon saturated dye solutions upon exposure (Tables 3 and 4). Alternatively, the methyl radicals could be formed by photoreduction of DMSO by photo-excited dye molecules [52].



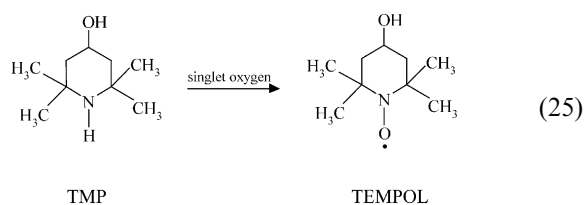
The continuous irradiation of C.I. Acid Red 87 (Eosin Y) and C.I. Basic Blue 9 (Methylene Blue) in DMSO/DMPO/Ar solutions caused the production of •DMPO–SR adduct, originating from solvent, as was described previously [42]. Furthermore, photoexcitation of the latter dye in DMSO/ND/Ar media resulted in the formation of three-line EPR signal ( $a_N = 0.730$  mT;  $g = 2.0045$ ), assigned to MB cation-radical, MB•<sup>+</sup>, produced by photoinduced electron transfer from the phenothiazine skeleton [50].

### 3.3. Singlet oxygen production upon irradiation of dyes evidenced by EPR

Photoexcited molecules of C.I. Acid Red 87 (Eosin Y) and C.I. Basic Blue 9 (Methylene Blue) in oxygenated media are defined as effective producers of singlet oxygen [53–56]. However, the

information on the ability of triarylmethane dyes to generate  $^1\text{O}_2$  upon photoexcitation found in literature is not consistent.

In our experiment, the formation of singlet oxygen upon irradiation of triarylmethane dyes was confirmed using the selective reaction of TMP with  $^1\text{O}_2$  [53,57,58], which resulted in the formation of stable nitroxyl free radical TEMPOL [Eq. (25)].



The application of TMP in oxygen-saturated solutions of triarylmethane dyes, as well as in

Table 3

Simulation parameters of EPR spectra for DMPO spin adducts obtained after 15 min of continuous irradiation ( $\lambda > 300$  nm) in argon-saturated DMSO solutions

Dye	DMPO spin adduct	Hyperfine splittings (mT)	g-value	Relative concentration (%)	Reference
C.I. Basic Red 9 (Basic Fuchsin)	•DMPO–OR	$a_{\text{N}} = 1.375$ $a_{\text{H}}^{\beta} = 1.324$	2.0059	84.4	[27, 49]
	•DMPO–CH <sub>3</sub>	$a_{\text{N}} = 1.480$ $a_{\text{H}}^{\beta} = 2.100$	2.0056	15.6	[27, 47]
C.I. Basic Green 4 (Malachite Green Oxalate)	•DMPO–CH <sub>3</sub>	$a_{\text{N}} = 1.480$ $a_{\text{H}}^{\beta} = 2.100$	2.0056	87.1	[27, 47]
	•DMPO–NR	$a_{\text{N}} = 1.288$ $a_{\text{H}}^{\beta} = 1.040$ $a_{\text{H}}^{\gamma} = 0.142$	2.0056	12.9	[27]
C.I. Basic Violet 3 (Crystal Violet)	•DMPO–CH <sub>3</sub>	$a_{\text{N}} = 1.478$ $a_{\text{H}}^{\beta} = 2.102$	2.0056	100	[27, 47]
C.I. Basic Blue 11 (Victoria Blue R)	•DMPO–O <sub>2</sub> <sup>•−</sup>	$a_{\text{N}} = 1.288$ $a_{\text{H}}^{\beta} = 1.040$ $a_{\text{H}}^{\gamma} = 0.142$	2.0059	77.0	[27, 42, 43]
	•DMPO–CH <sub>3</sub>	$a_{\text{N}} = 1.485$ $a_{\text{H}}^{\beta} = 2.080$	2.0056	7.2	[27, 47]
	•DMPO–SR	$a_{\text{N}} = 1.415$ $a_{\text{H}}^{\beta} = 1.190$	2.0058	15.8	[27, 49]
C.I. Acid Green 16	•DMPO–CH <sub>3</sub>	$a_{\text{N}} = 1.475$ $a_{\text{H}}^{\beta} = 2.095$	2.0056	31.0	[27, 47]
	•DMPO–O <sub>2</sub> <sup>•−</sup>	$a_{\text{N}} = 1.285$ $a_{\text{H}}^{\beta} = 1.040$ $a_{\text{H}}^{\gamma} = 0.147$	2.0059	32.0	[27, 42, 43]
	•DMPO–SR	$a_{\text{N}} = 1.400$ $a_{\text{H}}^{\beta} = 1.163$ $a_{\text{H}}^{\gamma} = 0.135$	2.0058	37	[27, 49]
C.I. Acid Blue 93	•DMPO–O <sub>2</sub> <sup>•−</sup>	$a_{\text{N}} = 1.290$ $a_{\text{H}}^{\beta} = 1.045$ $a_{\text{H}}^{\gamma} = 0.135$	2.0059	100	[27, 42, 43]
	•DMPO–OR	$a_{\text{N}} = 1.305$ $a_{\text{H}}^{\beta} = 1.491$	2.0059	62.7	[27, 49]
C.I. Basic Blue 9 (Methylene Blue)	•DMPO–CH <sub>3</sub>	$a_{\text{N}} = 1.472$ $a_{\text{H}}^{\beta} = 2.110$	2.0056	37.3	[27, 47]
	•DMPO–OR	$a_{\text{N}} = 1.444$ $a_{\text{H}}^{\beta} = 2.080$	2.0056	47.9	[27, 47]
C.I. Acid Red 87 (Eosin Y)	•DMPO–CH <sub>3</sub>	$a_{\text{N}} = 1.444$ $a_{\text{H}}^{\beta} = 2.080$	2.0056	47.9	[27, 47]
	•DMPO–OR	$a_{\text{N}} = 1.309$ $a_{\text{H}}^{\beta} = 1.505$	2.0059	33.2	[27, 49]
	semiquinone	$a_{\text{H}}(2\text{H}) = 0.340$	2.0056	18.9	[40, 41]

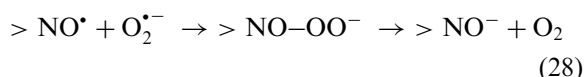
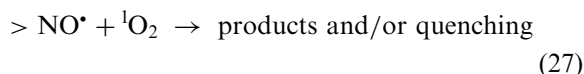
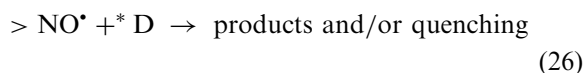
Table 4

Simulation parameters of EPR spectra for nitrosodurene spin adducts obtained after 15 min of continuous irradiation ( $\lambda > 300$  nm) in deoxygenated DMSO solutions saturated with spin trapping agent

Dye	ND spin adduct	Hyperfine splittings (mT)	<i>g</i> -value	Relative concentration (%)	Reference
C.I. Basic Red 9 (Basic Fuchsin)	•ND–CR •ND–CH <sub>3</sub>	$a_N = 1.318$ $a_N = 1.410$ $a_H^\beta(3H) = 1.282$	2.0057 2.0056	79 21	[27,39,46,47] [27,46,47]
C.I. Basic Green 4 (Malachite Green Oxalate)	•ND–CH <sub>3</sub>	$a_N = 1.408$ $a_H^\beta(3H) = 1.282$	2.0056	100	[27,46,47]
C.I. Basic Violet 3 (Crystal Violet)	•ND–CH <sub>3</sub>	$a_N = 1.410$ $a_H^\beta(3H) = 1.286$	2.0056	100	[27,46,47]
C.I. Basic Blue 11 (Victoria Blue R)	•ND–CR •ND–CH <sub>3</sub>	$a_N = 1.322$ $a_N = 1.410$ $a_H^\beta(3H) = 1.285$	2.0057 2.0056	5.8 94.2	[27,39,46,47] [27,46,47]
C.I. Acid Green 16	–	–	–	–	–
C.I. Acid Blue 93	•ND–CH <sub>3</sub>	$a_N = 1.413$ $a_H^\beta(3H) = 1.292$	2.0056	100	[27,46,47]
C.I. Basic Blue 9 (Methylene Blue)	MB• <sup>+</sup> •ND–CR •ND–CH <sub>3</sub>	$a_N = 0.730$ $a_N = 1.308$ $a_N = 1.395$ $a_H^\beta(3H) = 1.287$	2.0045 2.0057 2.0056	96 2 2	[50] [27,39,46,47] [27,46,47]
C.I. Acid Red 87 (Eosin Y)	•ND–CH <sub>3</sub>	$a_N = 1.405$ $a_H^\beta(3H) = 1.285$	2.0056	100	[27,46,47]

solutions of recognized <sup>1</sup>O<sub>2</sub> producers C.I. Basic Blue 9 (Methylene Blue) and C.I. Acid Red 87 (Eosin Y), showed evidence that singlet oxygen was produced upon irradiation of dyes only in dimethylsulphoxide. The experiments with TMP were unsuccessful, when deuterium oxide or ethanol solvents were applied, probably due to the short lifetime of singlet oxygen in these media [21].

Fig. 8 shows the time evolution of EPR spectra measured upon continuous irradiation of oxygen-saturated DMSO solutions of C.I. Acid Red 87 (Eosin Y) (Fig. 8a) and C.I. Basic Blue 9 (Methylene Blue) (Fig. 8b) in the presence of TMP. The EPR signal, corresponding to photooxidative generation of TEMPOL, increased significantly at the beginning of irradiation, then reached a maximum, but subsequently decreased with the prolonged irradiation time. This decline may be explained by the interaction of the photoproduct nitroxyl radical (TEMPOL) with photoexcited molecules of dyes [Eq. (26)] [59,60], as well as by the reactions with simultaneously produced singlet oxygen and super-oxide anion radicals [Eqs. (27 and (28))] [61–63].



The EPR spectra monitored upon photoexcitation of C.I. Acid Red 87 (Eosin Y)/DMSO/TMP/O<sub>2</sub> solution correspond to the formation of TEMPOL ( $a_N = 1.578$  mT;  $g = 2.0060$ ; Fig. 8a). However, upon photoexcitation of C.I. Basic Blue 9 (Methylene Blue)/DMSO/TMP/O<sub>2</sub> system, the experimental EPR spectra were attributed to two signals, and consequently simulated as a linear combination of signal corresponding to TEMPOL and additional three-line spectrum corresponding to MB•<sup>+</sup> ( $a_N = 0.702$  mT and  $g = 2.0045$ ).

The relative intensity of EPR signal reflecting photooxidative TEMPOL formation upon irradiation of triarylmethane dyes is significantly lower comparing to C.I. Acid Red 87 (Eosin Y) and C.I. Basic Blue 9 (Methylene Blue), as is depicted in Fig. 9. Extremely low intensities of this EPR signal were measured upon photoexcitation of C.I. Basic Green 4 (Malachite Green Oxalate) and C.I. Acid Green 16 (Fig. 9). However, due to the possible transformations of nitroxyl groups [Eqs. (26)–(28)], we could not exclude  $^1\text{O}_2$  also

being formed upon photoexcitation of these triarylmethane dyes.

### 3.4. Photooxidation processes of dyes investigated using TEMPOL termination

The ability of photogenerated reactive species to reduce the EPR signal of nitroxyl radicals was tested using oxygenated DMSO dye solutions by addition of TEMPOL [64]. Fig. 10a represents the dependence of the TEMPOL relative EPR signal

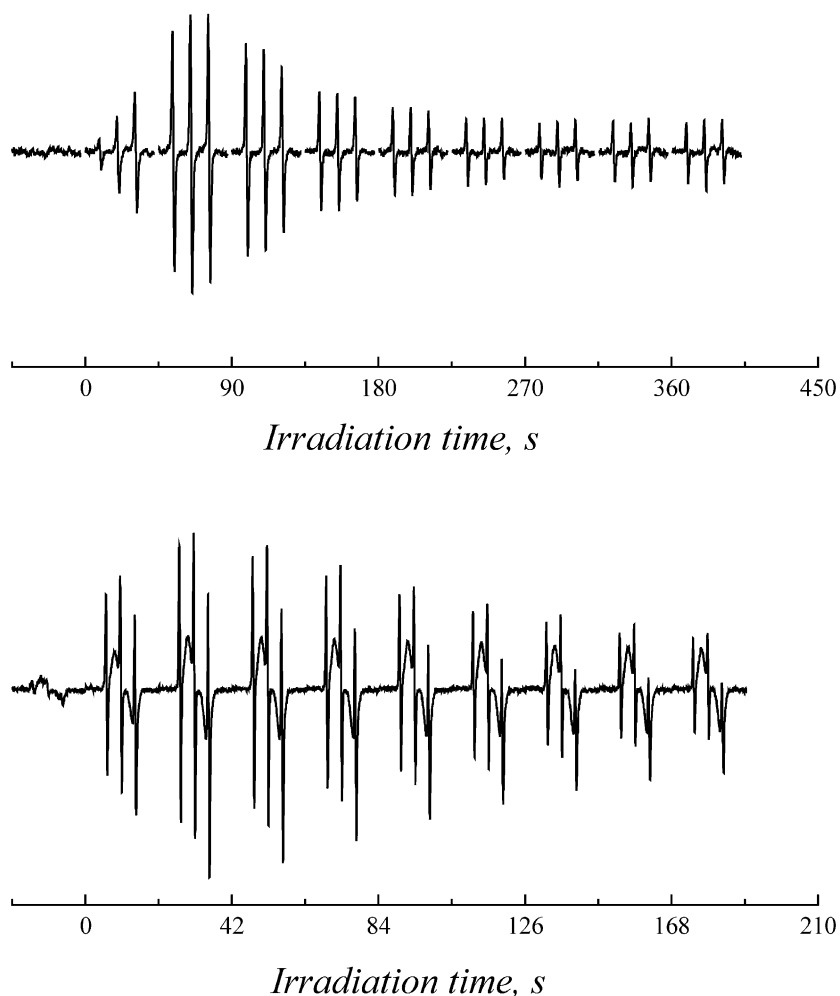
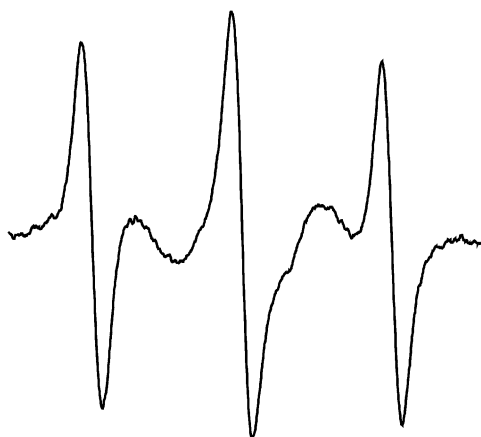


Fig. 8. Time evolution of EPR spectra (sweep width of 6 mT) measured upon continuous irradiation ( $\lambda > 300$  nm) of oxygen-saturated DMSO solutions in the presence of TMP ( $c_{\text{TMP}} = 0.001 \text{ mol dm}^{-3}$ ): (a) C.I. Acid Red 87 (Eosin Y) ( $c_{\text{dye}} = 4.0 \times 10^{-4} \text{ mol dm}^{-3}$ ); (b) C.I. Basic Blue 9 (Methylene Blue) ( $c_{\text{dye}} = 7.4 \times 10^{-4} \text{ mol dm}^{-3}$ ).

***C.I. Basic Red 9******C.I. Acid Green 16******C.I. Basic Green 4******C.I. Basic Blue 11******C.I. Basic Violet 3******C.I. Acid Blue 93***

345 346 347 348 349 350

*Magnetic field, mT*

345 346 347 348 349 350

*Magnetic field, mT*

Fig. 9. Experimental EPR spectra measured upon 10 min of continuous irradiation ( $\lambda > 300$  nm) in oxygen-saturated dye/DMSO/TMP solutions ( $c_{\text{TMP}} = 0.001 \text{ mol dm}^{-3}$ ;  $\rho_{\text{dye}} = 0.275 \text{ mg cm}^{-3}$ ).

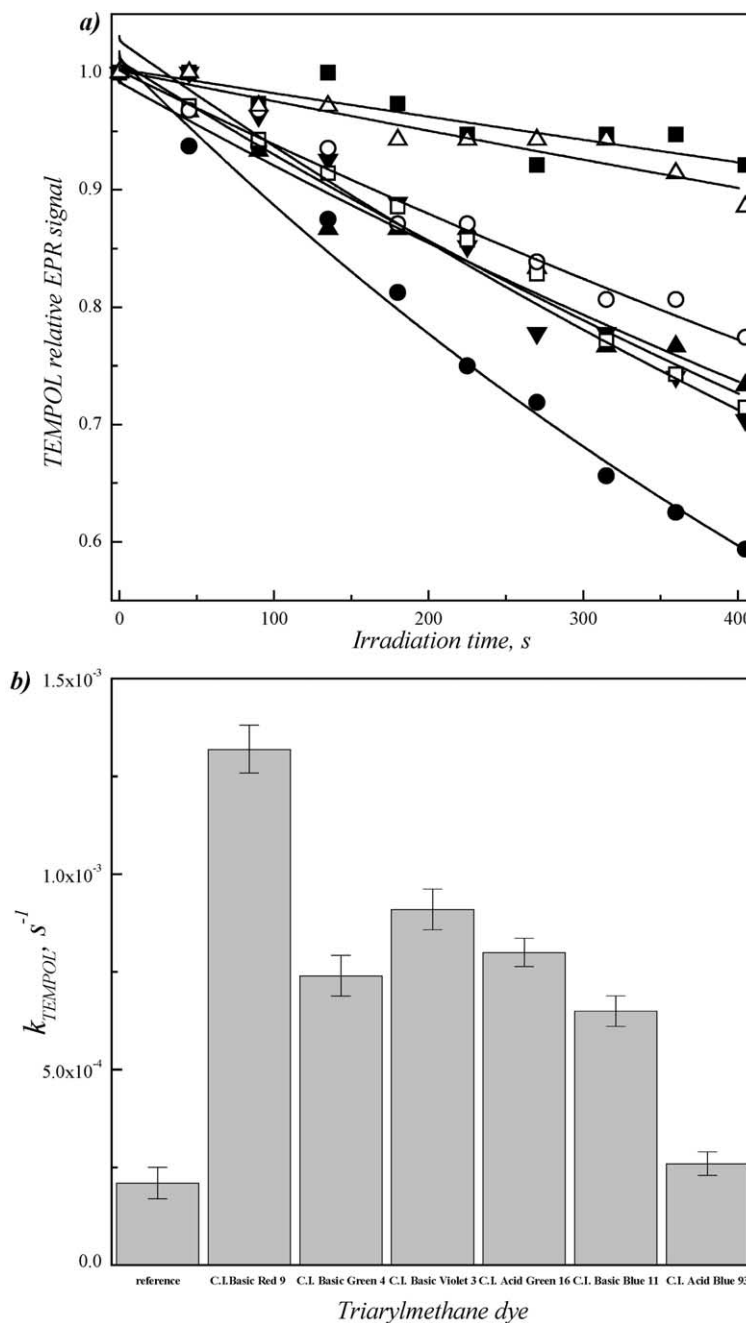


Fig. 10. (a) The dependence of TEMPOL relative EPR signal on irradiation time determined in the irradiated oxygen-saturated DMSO solutions in the presence of TEMPOL ( $c_{\text{TEMPOL}} = 0.16 \mu\text{mol dm}^{-3}$ ;  $\rho_{\text{dye}} = 0.32 \text{ mg cm}^{-3}$ ): Reference (■); C.I. Basic Red 9 (Basic Fuchsin) (●); C.I. Basic Green 4 (Malachite Green Oxalate) (▲); C.I. Basic Violet 3 (Crystal Violet) (▼); C.I. Acid Green 16 (□); C.I. Basic Blue 11 (Victoria Blue R) (○); C.I. Acid Blue 93 (△). The solid lines represent the mathematical simulations of experimental data in accord with the formal first-order kinetics. (b) The formal first-order rate constants,  $k_{\text{TEMPOL}}$ , with standard deviations calculated using least square analysis of TEMPOL relative EPR signal decline on irradiation time in oxygen-saturated dye/DMSO/TEMPOL solutions ( $c_{\text{TEMPOL}} = 0.16 \mu\text{mol dm}^{-3}$ ;  $\rho_{\text{dye}} = 0.32 \text{ mg cm}^{-3}$ ).

on the irradiation time in the solutions containing triarylmethane dye/DMSO/TEMPOL/O<sub>2</sub>, as well as in the reference system without dye. From the experimental spectra we measured the intensity of TEMPOL EPR signal for the individual irradiation periods, and consequently, TEMPOL relative EPR signal,  $I_{\text{EPR}}(\text{TEMPOL})$ , was calculated according to [Eq. (29)]:

$$I_{\text{EPR}}(\text{TEMPOL}) = \frac{I_t(\text{TEMPOL})}{I_0(\text{TEMPOL})} \quad (29)$$

where  $I_0(\text{TEMPOL})$  represents the initial EPR intensity of TEMPOL and  $I_t(\text{TEMPOL})$  corresponds to the free radical EPR signal after various irradiation periods.

The experimental data were plotted as the exponential function (solid lines in Fig. 10a) using least square analysis (program Scientist, Micro-Math) and the corresponding values of formal first-order rate constant ( $k_{\text{TEMPOL}}$ ) were calculated. The statistic parameters of fitting calculations (sum of square deviations, *R*-squared, correlation, coefficient of determination) showed good agreement of the experimental and calculated data. The calculated values of the formal first-order rate constant representing the decrease of TEMPOL relative to EPR intensity in the irradiated dye solutions are shown in Fig. 10b. The highest values of  $k_{\text{TEMPOL}}$  were established upon illumination of symmetrical dyes C.I. Basic Red 9 (Basic Fuchsin) and C.I. Basic Violet 3 (Crystal Violet), but only negligible decline, comparable with blank experiment, was demonstrated in the presence of C.I. Acid Blue 93 (Fig. 10b).

### 3.5. Photooxidation of dyes on paper substrate

The properties of substrates (paper, polymer matrix) may significantly influence the photo-degradation processes of dyes initiated by irradiation. Additionally, the radical species produced upon the photoexcitation of dyes can initiate deterioration processes of substrates, leading to the loss of mechanical and optical properties [14–20].

In attempt to evidence the production of reactive oxygen species (O<sub>2</sub><sup>•-</sup>, <sup>1</sup>O<sub>2</sub>) upon irradiation of the investigated dyes on solid substrate, we pre-

pared coloured paper samples using ethanolic solutions of dyes, DMPO or TMP. After spontaneous evaporation of solvent in the dark, we irradiated the tinted paper directly in the cavity of the EPR spectrometer and monitored the EPR spectra in situ. Fig. 11 represents the EPR spectra observed after 10 min of continuous irradiation of paper coloured by C.I. Acid Blue 93 (Fig. 11a) and C.I. Acid Red 87 (Eosin Y) (Fig. 11b) in the presence of TMP. These data clearly demonstrate the photoinduced formation of singlet oxygen and photooxidation of TMP generating paramagnetic TEMPOL. The anisotropy of the EPR spectra resulted from the motionally restricted nitroxyl group of TEMPOL in the paper matrix. The analogous experiments performed using DMPO spin trapping agent led to the photoinitiated formation

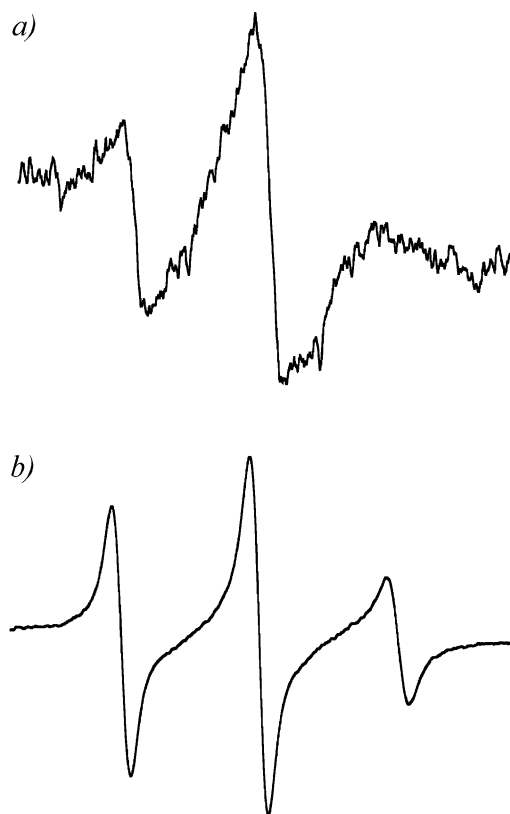


Fig. 11. Experimental EPR spectra measured upon 10 min of continuous irradiation ( $\lambda > 300$  nm) of coloured paper in the presence of TMP: (a) C.I. Acid Blue 93; (b) C.I. Acid Red 87 (Eosin Y).

of an anisotropic four-line signal corresponding to  $\bullet\text{DMPO-O}_2^-$ , though the EPR intensity of signal was low.

#### 4. Conclusions

The results of EPR investigations of six triarylmethane dyes (C.I. Basic Red 9 (Basic Fuchsin), C.I. Basic Green 4 (Malachite Green Oxalate), C.I. Basic Violet 3 (Crystal Violet), C.I. Acid Green 16, C.I. Basic Blue 11 (Victoria Blue R), C.I. Acid Blue 93), as well as C.I. Basic Blue 9 (Methylene Blue) and C.I. Acid Red 87 (Eosin Y) may be summarized as follows:

- The EPR spectra of original polycrystalline dye samples measured at 290 K are characterized by anisotropic paramagnetic signals at  $g_{\text{eff}} = 2.0044$ , which were attributed to the peroxidic intermediates produced by the autoxidation processes. The highest autoxidation deterioration was observed for dyes, which evidenced the most efficient production of singlet oxygen. The presence of peroxidic intermediates plays an important role in the photochemical transformations of dyes especially under anaerobic conditions.
- The excitation of oxygenated aqueous solutions of C.I. Basic Green 4 (Malachite Green Oxalate), C.I. Basic Violet 3 (Crystal Violet), C.I. Acid Green 16 and C.I. Basic Blue 9 (Methylene Blue) in the presence of a DMPO spin trap resulted in the formation of an EPR signal corresponding to the  $\bullet\text{DMPO-OH}$  adduct. The photochemical excitation of ethanolic solutions of dyes led to the formation of reactive radical species in both argon- or oxygen-saturated systems, which were identified by means of DMPO and ND spin trapping agents.
- Irradiation of triarylmethane dyes in argon-saturated DMSO solutions in the presence of DMPO and ND initiated the generation of various radical products evidenced as the corresponding spin adducts. Under oxygen, the effective electron transfer from the

photoexcited dye molecules to oxygen was confirmed.

- The application of a selective agent for singlet oxygen detection (TMP) brought evidence on the efficient formation of  $^1\text{O}_2$  in the irradiated DMSO solutions of C.I. Basic Blue 9 (Methylene Blue) and C.I. Acid Red 87 (Eosin Y), and additionally in the majority of triarylmethane dyes.
- The EPR experiments confirmed the effective formation of super-oxide anion radical and singlet oxygen upon photoexcitation of paper substrate coloured using investigated dyes in the presence of corresponding detection reagent (DMPO or TMP).
- The efficient protection of archival documents containing inks prepared from triarylmethane dyes, C.I. Basic Blue 9 (Methylene Blue) and C.I. Acid Red 87 (Eosin Y) requires strict elimination of light and oxygen.

#### Acknowledgements

We thank Slovak Grant Agency (Projects VEGA/1/0053/03 and VEGA/1/9145/02) for financial support.

#### References

- [1] Zollinger H. Color chemistry. Syntheses, properties and applications of organic dyes and pigments. Weinheim: VCH; 1991.
- [2] Ullmann's Encyclopedia of Industrial Chemistry. Part A27. Triarylmethane and Diarylmethane Dyes. 6th ed. New York: Wiley-VCH; 2001.
- [3] Available: <http://members.pgonline.com/~bryand/StainsFile/>.
- [4] Bhasikuttan AC, Sapre AV, Shastri LV. Photoinduced electron transfer in crystal violet ( $\text{CV}^+$ )-bovine serum albumin (BSA) system: evaluation of reaction paths and radical intermediates. *J Photochem Photobiol A: Chem* 2002;150:59–66.
- [5] Viola A, Hadjur C, Jeunet A, Julliard M. Electron paramagnetic resonance evidence of the generation of super-oxide ( $\text{O}_2^-$ ) and hydroxyl ( $\bullet\text{OH}$ ) radicals by irradiation of a new photodynamic therapy photosensitizer, Victoria Blue BO. *J Photochem Photobiol B: Biol* 1996;32:49–58.

- [6] Wainwright M, Burrow SM, Guinot SGR, Phoenix DA, Waring J. Uptake and cell-killing activities of a series of Victoria blue derivatives in a mouse mammary tumour cell line. *Cytotechnol* 1999;29:35–43.
- [7] Bonnett R, Martínez G. Photobleaching of sensitizers used in photodynamic therapy. *Tetrahedron* 2001;57: 9513–47.
- [8] Baptista MS, Indig GL. Effect of BSA binding on photo-physical and photochemical properties of triarylmethane dyes. *J Phys Chem B* 1998;102:4678–88.
- [9] Buettner GR, Doherty TP, Bannister TD. Hydrogen peroxide and hydroxyl radical formation by methylene blue in the presence of ascorbic acid. *Radiat Environ Biophys* 1984;23:235–43.
- [10] Lewis LM, Indig GL. Effect of dye aggregation on triarylmethane-mediated photoinduced damage of hexokinase and DNA. *J Photochem Photobiol B: Biol* 2002;67:139–48.
- [11] Kandela K, Bartlett JA, Indig GL. Effect of molecular structure on the selective phototoxicity of triarylmethane dyes towards tumor cells. *Photochem Photobiol Sci* 2002; 1:309–14.
- [12] Kowaltowski AJ, Turin J, Indig GL, Vercesi AE. Mitochondrial effects of triarylmethane dyes. *J Bioenerg Biomembr* 1999;31:581–90.
- [13] Feller RL. Accelerated aging. Photochemical and thermal aspects. The J. Paul Getty Trust; 1994.
- [14] Allen NS, McKellar JF, Mohajerani B. Lightfastness and spectroscopic properties of basic triphenylmethane dyes: effect of the substrate. *Dyes and Pigments* 1980;1:49–57.
- [15] Allen NS. Photofading and light-stability of dyed and pigmented polymers. *Polym Degr Stab* 1994;44:357–74.
- [16] Duxbury DF. The sensitized fading of triphenylmethane dyes in polymer films. Part 1. *Dyes and Pigments* 1994;25: 131–66.
- [17] Duxbury DF. The sensitized fading of triphenylmethane dyes in polymer films. Part 2. *Dyes and Pigments* 1994;25: 179–204.
- [18] Kawai H, Toshihiko N. Inverse photochromism of substituted triphenylmethane dyes in poly (vinyl alcohol) films. *J Photochem Photobiol A: Chem* 1995;92:105–9.
- [19] Oda H. Effect of phenyl ester UV absorbers bearing a singlet oxygen quencher on photofading of crystal violet in a polymer substrate. *Textile Res J* 2001;71:1057–62.
- [20] Abbott LC, MacFaul P, Jansen L, Oakes J, Lindsay Smith JR, Moore JM. Spectroscopic and photochemical studies of xanthene and azo-dyes on surfaces: cellophane as a mimic of paper and cotton. *Dyes and Pigments* 2001;48: 49–56.
- [21] Braun AM, Maurette MT, Oliveiros E. Technologie photochimique. Première ed. Lausanne: Presses polytechniques romandes; 1986.
- [22] Available: <http://www.brite-lite.com/Products/Suntanlamps.htm>.
- [23] Feller RL. Accelerated aging. Photochemical and thermal aspects. The J. Paul Getty Trust; 1994 (Appendix C).
- [24] Rånby B, Rabek JF. ESR spectroscopy in polymer research. Berlin: Springer-Verlag; 1977.
- [25] Denisov ET, Denisova TG, Pokidova TS. Handbook of free radical initiators. New York: Wiley; 2003.
- [26] Rosen GM, Britigan BE, Halpern HJ, Pou S. Free radicals: biology and detection by spin trapping. Oxford University Press; 1999.
- [27] Li ASW, Cummings KB, Roethling HP, Buettner GR, Chignell CF. A spin-trapping database implemented on the IBM PC/AT. *J Magn Reson* 1988;79:140–2 [available: <http://epr.niehs.nih.gov/stdb.html>].
- [28] Miller CM, Valentine RL. Mechanistic studies of surface catalyzed  $H_2O_2$  decomposition and contaminant degradation in the presence of sand. *Wat Res* 1999;33:2805–16.
- [29] Zhang H, Joseph J, Vasquez-Vivar J, Karoui H, Nsanzumuhire C, Martíásek P, Tordo P, Kalyanaraman B. Detection of superoxide anion using an isotopically labeled nitron spin trap: potential biological applications. *FEBS Lett* 2000;473:58–62.
- [30] Galindo C, Jacques P, Kalt A. Photodegradation of the aminoazobenzene acid orange 52 by three advanced oxidation processes: UV/ $H_2O_2$ , UV/ $TiO_2$  and VIS/ $TiO_2$ . Comparative mechanistic and kinetic investigations *J Photochem Photobiol A: Chem* 2000;130:35–47.
- [31] Zhang T, Oyama T, Horikoshi S, Hidaka H, Zhao J, Serpone N. Photocatalyzed N-demethylation and degradation of methylene blue in titania dispersions exposed to concentrated sunlight. *Solar Energy Mat Solar Cells* 2002; 73:287–303.
- [32] Zhang T, Oyama T, Aoshima A, Hidaka H, Zhao J, Serpone N. Photooxidative N-demethylation of methylene blue in aqueous  $TiO_2$  dispersions under UV irradiation. *J Photochem Photobiol A: Chem* 2001;140:163–72.
- [33] Saquib M, Muneer M.  $TiO_2$ -mediated photocatalytic degradation of a triphenylmethane dye (gentian violet), in aqueous suspensions. *Dyes and Pigments* 2003;56:37–49.
- [34] Caine MA, McCabe RW, Wang L, Brown RG, Hepworth JD. The influence of singlet oxygen in the fading of carbonless copy paper primary dyes on clays. *Dyes and Pigments* 2001;49:135–43.
- [35] Gadelha FR, Hanna PM, Mason RP, Docampo R. Evidence for free radical formation during horseradish peroxidase-catalyzed N-demethylation of crystal violet. *Chem Biol Interact* 1992;85:35–48.
- [36] Ferreira-Leitão VS, da Silva JG, Bon EPS. Methylene blue and azure B oxidation by horseradish peroxidase: a comparative evaluation of class II and class III peroxidases. *Appl Catal B: Environ* 2003;42:213–21.
- [37] Alegría AE, Ferrer A, Santiago G, Sepúlveda E, Flores W. Photochemistry of water-soluble quinones. Production of the hydroxyl radical, singlet oxygen and the superoxide ion. *J Photochem Photobiol A: Chem* 1999;127:57–65.
- [38] Brezová V, Staško A, Biskupič S. Radical intermediates in the photochemical decomposition of *p*-toluenesulphonate (a kinetic spin trapping study). *J Photochem Photobiol A: Chem* 1993;71:229–35.
- [39] Brezová V, Tarábek P, Dvoranová D, Staško A, Biskupič S. EPR study of photoinduced reduction of nitroso com-

- pounds in titanium dioxide suspensions. *J Photochem Photobiol A: Chem* 2003;155:179–98.
- [40] Ajtai K, Burghardt TP. Luminescent paramagnetic probes for detecting order in biological assemblies—transformation of luminescent probes into  $\pi$ -radicals by photochemical reduction. *Biochem* 1992;31:4275–82.
- [41] Marchesi E, Rota C, Fann IC, Chignell CF, Mason RP. Photoreduction of fluorescent dye 2'-7'-dichlorofluorescein: a spin trapping and direct electron spin resonance study with implications for oxidative stress measurements. *Free Radic Biol Med* 1999;26:148–61.
- [42] Noda H, Oikawa K, Ohya-Nishiguchi H, Kamada H. Detection of superoxide ions from photoexcited semiconductors in non-aqueous solvents using the ESR spin-trapping technique. *Bull Chem Soc Jpn* 1993;66:3542–7.
- [43] Calle P, Fernández-Arizpe A, Sieiro C. Photosensitization by Harmine: an ESR spin trapping study on the generation of the superoxide anion radical. *Appl Spec* 1996;50:1446–51.
- [44] Yoshimuri Y, Inomata T, Nakazawa H. Simultaneous detection of superoxide anion, hydroxyl radical, and methyl radical by use of high performance liquid chromatography–electron spin resonance. *J Liq Chrom Rel Technol* 1999;22:419–28.
- [45] Bilski P, Reszka K, Bilski M, Chignell CF. Oxidation of spin trap 5,5-dimethyl-1-pyrroline *N*-oxide by singlet oxygen in aqueous solution. *J Am Chem Soc* 1996;118:1330–8.
- [46] Forrester AR in: Landolt-Börnstein. Numerical data and functional relationships in science and technology. New series (Ed. in chief Madelung O), Group II: atomic and molecular physics. Volume 17: magnetic properties of free radicals. Subvolume d1: nitroxide radicals Part I (Ed. Fischer H). Berlin: Springer; 1989, pp. 268.
- [47] Staško A, Erentová K, Raptá P, Nyuken O, Voit B. Investigation of the decomposition of compounds containing azo group by EPR spectroscopy. *Magn Reson Chem* 1998;36:13–34.
- [48] Maldotti A, Andreotti L, Molinari A, Tollari S, Penoni A, Cenini S. Photochemical and photocatalytic reduction of nitrobenzene in the presence of cyclohexene. *J Photochem Photobiol A: Chem* 2000;133:129–33.
- [49] Rojas Wahl RU, Zeng L, Madison S, DePinto RL, Shay BJ. Mechanistic study of decomposition of water soluble azo-radical-initiators. *J Chem Soc Perkin Trans* 1998;2:2009–17.
- [50] Turro NJ, Khudyakov IV, van Willigen H. Photoionization of phenothiazine: EPR detection of reactions of the polarized solvated electron. *J Am Chem Soc* 1995;117:12273–80.
- [51] Woodward JR, Lin TS, Sakaguchi Y, Hayashi H. Detection of transient intermediates in the photochemical reaction of hydrogen peroxide with dimethyl sulfoxide by time-resolved EPR techniques. *J Phys Chem A* 2000;104:557–61.
- [52] Alegría AE, Krishna CM, Elespuru RK, Riesz P. An ESR study of the visible light photochemistry of gilvocarcin V. *Photochem Photobiol* 1989;49:257–65.
- [53] Zang LY, van Kuijk FJGM, Misra BR, Misra HP. The specificity and product of quenching singlet oxygen by 2,2,6,6-tetramethylpiperidine. *Biochem Mol Biol Inter* 1995;37:283–93.
- [54] Wainwright M, Phoenix DA, Rice L, Burrow SM, Waring J. Increased cytotoxicity and phototoxicity in the methylene blue series via chromophore methylation. *J Photochem Photobiol B: Biol* 1997;40:233–9.
- [55] Kuramoto N, Kitao T. The contribution of singlet oxygen to the photofading of triphenylmethane and related dyes. *Dyes and Pigments* 1982;3:49–58.
- [56] Arakane K, Ryu A, Takaranda K, Masunaga T, Shinmoto K, Kobayashi R, et al. Measurements of 1268 nm emission for comparison of singlet oxygen ( $^1\Delta_g$ ) production efficiency of various dyes. *Chem Pharm Bull* 1996;44:1–4.
- [57] Li Y, Wang Q, Guo J, Wu G. ESR studies on the interaction of calixarenes and free radicals. *Mat Sci Eng C* 1999;10:25–8.
- [58] Ma L, Wang X, Wang B, Chen J, Wang J, Huang K, et al. Photooxidative degradation mechanism of model compounds of poly(p-phenylenevinylene)s [PPVs]. *Chem Phys* 2002;285:85–94.
- [59] Available: <http://www.rcdc.nd.edu/>.
- [60] Seret A, Gandin E, Van den Vorst A. Nitroxide reduction by electron transfer from the eosin triplet state: electron paramagnetic resonance and flash photolysis studies. *J Photochem* 1987;38:145–55.
- [61] Kishioka S, Umeda M, Yamada A. Effect of oxygen on the electrochemical reduction of nitroxyl radical: interpretation of the mechanism for a redox probe in biological systems. *Anal Sci* 2002;18:1379–81.
- [62] Samuni A, Mitchell JB, DeGraff W, Krishna CM, Samuni U, Russo A. Nitroxide SOD-mimics: modes of action. *Free Radic Res Commun* 1991;12–13:187–94.
- [63] Belford RE, Seely GR, Gust D, Moore TA, Moore A, Cherepy NJ, et al. Nitroxyl free radical enhancement of the forbidden  $O_2(^3\Sigma_g^-) \leftarrow O_2(^1\Delta_g)$  radiative transition in chlorinated hydrocarbon solvents. *J Photochem Photobiol A: Chem* 1993;70:125–33.
- [64] Feller RL. Accelerated aging. Photochemical and thermal aspects. The J. Paul Getty Trust; 1994 [Appendix E].